Discrete Diagonal State Estimator based Current Control for Grid Connected PWM Converter with an LCL filter

Byeong-Heon Kim†, Heonyoung Kim and Subhashish Bhattacharya*
FREEDM System Center
North Carolina Stae University
Raleigh, USA
†heon13@snu.ac.kr, *sbhatta4@ncsu.edu

***Abstract*—In this paper, the control and state observer for grid connected PWM converter with LCL filter has been discussed. The discrete state-space observer is designed in the *d-q* synchronous reference frame. Using the coordinate change of the matrix, the alternative state equation, which has diagonal system matrix, is obtained. Discretization of alternative state equation using Zero-Order Hold method is suggested, and the discrete form is simpler than that derived by original system matrix. By considering control stability with respect to the relation between filter resonant frequency and sampling frequency, current control scheme with feedback signal from state observer is also proposed. The digital delay to the PWM and sampling is considered for digital implementations.**

Keywords—LCL filter, digital observer, discrete time domain, control stability, resonant frequency, grid-connected converter.

I. Introduction

In grid-connected power conditioning system (PCS), fulfillment for current harmonic restriction is one of the critical issues. Accordingly harmonic filters are mainly inserted between the grid and PWM converters to reduce harmonic components from PWM switching [1]. LCL filters are more popularly used in various applications compared to L filters as higher inductance, which increases overall filter volume and weight, is required for L filters than the case for LCL filters [1]-[5]. However, a disadvantage of the LCL filter is the resonant behavior, and it could invoke instability of the system.

To suppress the resonance, passive or active damping technique has widely discussed. The resonance can be damped by a suitable resistor in passive damping, but the passive methods introduce losses in the system [2]. Active damping schemes are implemented by modifying the control loop [4]. However, in most cases, PCS requires additional sensors to implement active damping, and it increases cost and decreases system reliability. Some literature show that the digital time delay affects the LCL filtered system stability [5]-[7]. Appropriate selection of the position of current sensing and the ratio of the LCL resonant frequency (f_{res}) to sampling frequency (f_{samp}) allow to operate system in stable without any damping technique. In short, if f_{res} / f_{samp} is lower than 1/6, converter-side current should be fed-back for stable operation without damping scheme. By contrast, if f_{res} / f_{samp} is beyond 1/6, grid current for feedback signal will stabilize the system.

When using LCL filter, the current sensor for the current feedback in control can be placed either at the converter output or the filter output. Although the output power of PCS at the grid side should be controlled, in some cases, the current sensor should be installed at the output of the converter due to the package limitation. For small scale power system, shunt resistor can be adopted to sense current. For large scale system, it is hard to place current sensor at the grid side because the LCL filter size is getting larger and the feedback signal path from sensor to controller is getting longer and is more sensitive to noise. If such system set f_{res} / f_{samp} beyond 1/6 to reduce filter size, the active damping should be adopted and additional sensor should be installed. The notch filter based technique was also introduced to make phase margin without additional sensor, but it should consider frequency deviation from nominal value [4]. In [8], a discrete time observer based state-space current controller could operate system in stable without any damping technique although the f_{res} / f_{samp} was beyond 1/6, and the converter current was fed-back. However, the analytical gain for current control was much more complicated than conventional current controller. The active damping based on state observer was presented for LCL filter [9] without additional sensor. However, because these discrete state observer neglects loss component, they suffer from internal stability issues.

This paper presents control scheme based on state observer to stably operate LCL filtered system although the converter current is fed-back and the f_{res} / f_{samp} is beyond 1/6. In the previous paragraph, it was figured out that additional sensors was not mandatory to stabilize the system with unstable condition as described in previous literatures. The main contribution is adopting conventional synchronous reference frame proportional-integral (PI) regulator for current control and suggesting less complicate discrete time domain observer design. The state observer estimates grid currents, and these will be fed-back to controller for stable operation. To simplify discretization, the state equation is changed to the alternative diagonal system by similar transformation. The proposed alternative diagonal system can make system internally stable. The observer gains are set in discrete time domain. For the

978-1-4799-7312-5/18/$31.00 ©2018 IEEE

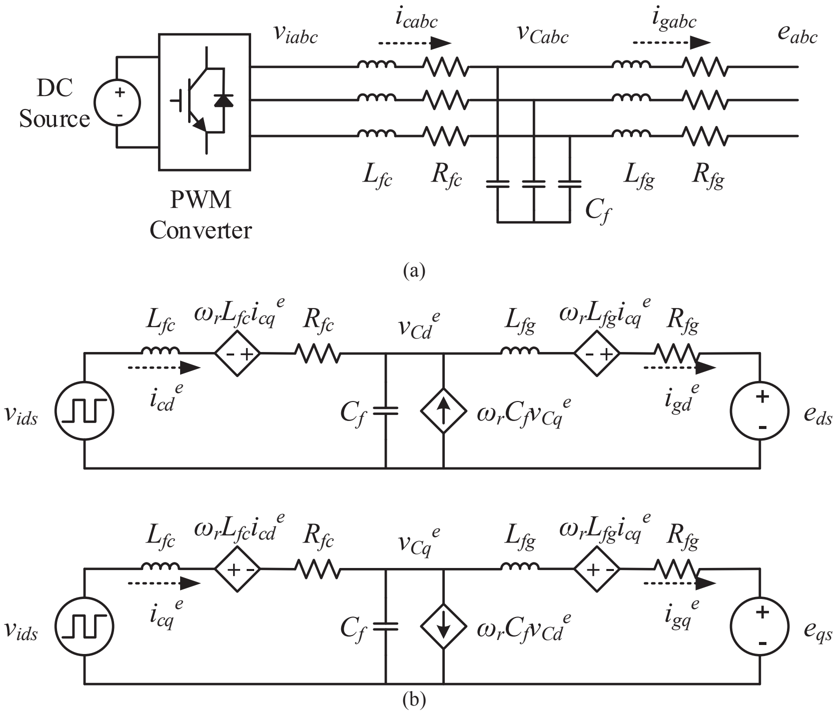

Fig. 1. (a) System configuration (b) *d-q* synchronous reference frame equivalent circuit

digital implementation, the voltage compensation considering digital delay is discussed.

In Section II, alternative diagonal system equation will be presented. This alternative system will be changed to discrete system equation using Zero-Order Hold (ZOH). In Section III, the observer gains will be set by the direct pole placement in discrete time domain. In addition, the control scheme without damping technique will be proposed based on conventional current regulator and state observer.

II. Alternative Discrete State Equation

A. Diagonalization

Fig. 1 (a) shows the system configuration for grid connected PCS with LCL filter, and the equivalent circuit can be depicted in *d-q* synchronous reference frame as in Fig. 1 (b). Complex space vectors in *d-q* synchronous coordinates are used as in [8] and [9]. In this paper, the grid voltage vector is aligned on the *q*-axis and the *q*-axis current is defined as an active power component [10]. The state equation can be represented as (1).

$$\begin{aligned}\dot{\mathbf{x}} &= \mathbf{A}\mathbf{x} + \mathbf{B}\mathbf{u} \\ \mathbf{y} &= \mathbf{C}\mathbf{x} + \mathbf{D}\mathbf{u}\end{aligned} \tag{1}$$

$$\text{where, } \mathbf{A} = \begin{bmatrix} -R_{fc}L_{fc}^{-1} - j\omega_g & -L_{fc}^{-1} & 0 \\ C_f^{-1} & -j\omega_g & -C_f^{-1} \\ 0 & -L_{fg}^{-1} & -R_{fg}L_{fg}^{-1} - j\omega_g \end{bmatrix},$$

$$\mathbf{B} = \begin{bmatrix} L_{fc}^{-1} & 0 & 0 \\ 0 & 0 & -L_{fg}^{-1} \end{bmatrix}^T, \ \mathbf{C} = \begin{bmatrix} 1 & 0 & 0 \end{bmatrix}, \ \mathbf{D} = \mathbf{0},$$

$$\mathbf{x} = \begin{bmatrix} \vec{i}_{cdq}^{\,e} & \vec{v}_{Cdq}^{\,e} & \vec{i}_{gdq}^{\,e} \end{bmatrix}^T, \ \mathbf{u} = \begin{bmatrix} \vec{v}_{idq}^{\,e} & \vec{e}_{dq}^{\,e} \end{bmatrix}^T, \ \mathbf{y} = \vec{i}_{cdq}^{\,e}.$$

In the aforementioned equations, R_{fc} and R_{fg} stand for the resistance of converter side and grid side filter inductor. L_{fc} and L_{fg} stand for the inductance of filter. C_f stands for the filter capacitance. ω_g stands for the grid frequency. $\vec{i}_{cdq}^{\,e}$, $\vec{v}_{Cdq}^{\,e}$ and $\vec{i}_{gdq}^{\,e}$ represent converter side current, filter capacitor voltage, and grid side current, respectively. $\vec{v}_{idq}^{\,e}$ and $\vec{e}_{dq}^{\,e}$ stand for converter output voltage and grid voltage respectively. The arrow on variables represents complex vector.

For implementation in digital signal processor, the system has to be discretized using several methods such as Euler's backward, Trapezoidal, or Zero-Order Hold methods, and these method maintain stability of the original system [11]. However, the inverse or exponential of the original state equation, which is essential factor to get stable discrete equation, have complex form, and it can be obstacle for implementation in practical.

To alleviate the computational burden, the original state equation could be changed to diagonal matrix using similar transformation [12], [13]. With lossless assumption, the change of coordinate matrix can be obtained as (2) [8]. The state equation can be written in alternative state equation as (3) by similar transformation with the state change as (4).

$$\mathbf{Q}=\begin{bmatrix} -L_{fg}L_{fc}^{-1} & 1 & -L_{fg}L_{fc}^{-1} \\ -j\omega_p L_{fg} & 0 & j\omega_p L_{fg} \\ 1 & 1 & 1 \end{bmatrix} \quad (2)$$

$$\begin{aligned} \dot{\bar{\mathbf{x}}} &= \bar{\mathbf{A}}\bar{\mathbf{x}}+\bar{\mathbf{B}}\mathbf{u} \\ \mathbf{y} &= \bar{\mathbf{C}}\bar{\mathbf{x}}+\bar{\mathbf{D}}\mathbf{u} \end{aligned} \quad (3)$$

$$\mathbf{x}=\mathbf{Q}\bar{\mathbf{x}} \quad (4)$$

where, $\bar{\mathbf{A}}=\mathbf{Q}^{-1}\mathbf{A}\mathbf{Q}=diag\left[\lambda_1 \quad \lambda_2 \quad \lambda_3\right]$,

$$\bar{\mathbf{B}}=\mathbf{Q}^{-1}\mathbf{B}=\frac{1}{L_{f,sum}}\begin{bmatrix} -\frac{1}{2} & -\frac{L_{fc}}{2L_{fg}} \\ 1 & -1 \\ -\frac{1}{2} & -\frac{L_{fc}}{2L_{fg}} \end{bmatrix},\ \bar{\mathbf{C}}=\mathbf{C}\mathbf{Q}=\begin{bmatrix} -\frac{L_{fg}}{L_{fc}} \\ 1 \\ -\frac{L_{fg}}{L_{fc}} \end{bmatrix}^T,$$

$\bar{\mathbf{D}}=\mathbf{D}=\mathbf{0}$, $L_{f,sum}=L_{fc}+L_{fg}$, and λ_i $(i=1, 2, 3)$ represents eigenvalue.

However, the original system with resistor cannot be changed to diagonal matrix by (2). In addition, the poles of alternative state equation derived with lossless assumption are placed in imaginary axis of Laplace domain, and the response of the system would be oscillated. This implies the system is internally unstable.

To avoid such oscillatory response in the system, asymptote eigenvalues has been proposed. The characteristic equation of the original system is represented as (5).

$$\begin{aligned} &\det(s\mathbf{I}-\mathbf{A}) \\ &=\left(s+j\omega_g+\omega_{LRc}\right)\left[\left(s+j\omega_g\right)\left(s+\omega_{LRg}+j\omega_g\right)+\omega_{LCg}^2\right] \\ &\quad +\omega_{LCc}^2\left(s+\omega_{LRg}+j\omega_g\right) \end{aligned} \quad (5)$$

where, $\omega_{LCc}=1/\sqrt{L_{fc}C_f}$, $\omega_{LCg}=1/\sqrt{L_{fg}C_f}$, $\omega_{LRc}=R_{fc}/L_{fc}$, and $\omega_{LRg}=R_{fg}/L_{fg}$.

Because the poles by inductors and resistors, ω_{LRc} and ω_{LRg}, are placed much lower than the poles by inductors and capacitor, ω_{LCc} and ω_{LCg}, (5) can be simplified to (6). The approximated characteristic equation gives the asymptote eigenvalues as (7).

$$\begin{aligned} &\det(s\mathbf{I}-\mathbf{A}) \\ &=\left(s+j\omega_g+\omega_{LR,avg}\right)\left[\left(s+j\omega_g+\frac{1}{2}\omega_{LR,avg}\right)^2+\omega_p^2\right] \end{aligned} \quad (6)$$

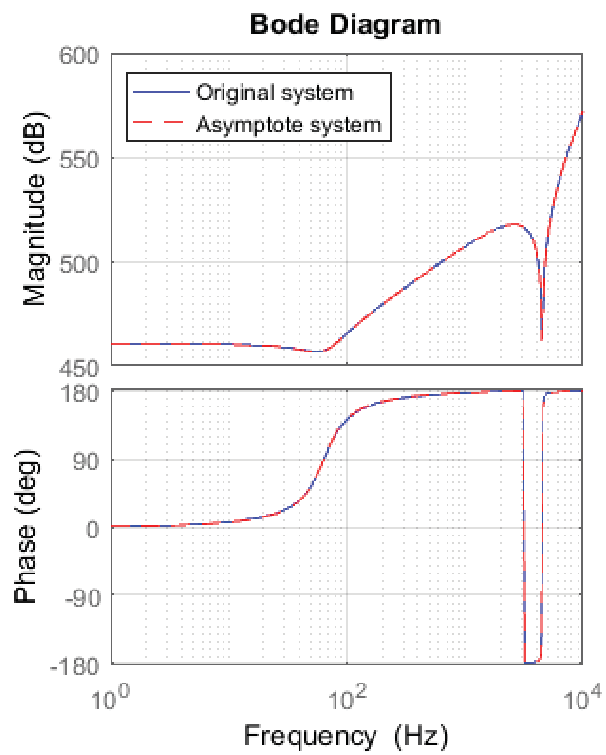

Fig. 2. Transfer function of system characteristic equations

$$\begin{aligned} \lambda_1 &= -j\left(\omega_g+\omega_p\right)-\frac{1}{2}\omega_{LR,avg} \\ \lambda_2 &= -j\omega_g-\omega_{LR,avg} \\ \lambda_3 &= -j\left(\omega_g-\omega_p\right)-\frac{1}{2}\omega_{LR,avg} \end{aligned} \quad (7)$$

where, $\omega_p=1/\sqrt{L_pC_f}$, $L_p=L_{fc}\parallel L_{fg}$, $\omega_{LR,avg}=\frac{1}{2}\left(\omega_{LRc}+\omega_{LRg}\right)$.

The diagonal elements of the system matrix ($\bar{\mathbf{A}}$) can be changed to the value in (7), and this diagonal matrix is valid with subtle errors. Fig. 2 shows the transfer function comparison of system characteristic equation between original system and diagonal system using asymptote eigenvalue. The error is negligible, and the asymptote pole can demonstrate the system dynamics without oscillations.

B. Discretization using Zero-Order Hold

Because the resonant frequency of LCL filter is affected by digital implementation, the state model for observer design in continuous time is not valid in digital processor. The state equation should be digitalized, and the state observer should be designed in discrete domain. The system has been discretized with the Zero-Order Hold (ZOH) method as (8) [8]-[9], [11]-[12].

$$\bar{\mathbf{x}}[k+1]=\bar{\mathbf{A}}_d\bar{\mathbf{x}}[k]+\bar{\mathbf{B}}_d\mathbf{u}[k]$$
$$\mathbf{y}[k]=\bar{\mathbf{C}}_d\bar{\mathbf{x}}[k]+\bar{\mathbf{D}}_d\mathbf{u}[k] \tag{8}$$

where, $\bar{\mathbf{A}}_d=e^{\bar{\mathbf{A}}T_s}=diag\left[\exp(\lambda_1T_s)\quad\exp(\lambda_2T_s)\quad\exp(\lambda_3T_s)\right]$,

$$\bar{\mathbf{B}}_d=\left(\int_0^{T_s}\exp\left(\bar{\mathbf{A}}\alpha\right)d\alpha\right)\bar{\mathbf{B}}$$

$$=\frac{1}{L_{f,sum}}\begin{bmatrix}-\frac{\exp(\lambda_1T_s)-1}{2\lambda_1} & -\frac{L_{fc}\left[\exp(\lambda_1T_s)-1\right]}{2L_{fg}\lambda_1}\\ \frac{\exp(\lambda_2T_s)-1}{\lambda_2} & \frac{\exp(\lambda_2T_s)-1}{\lambda_2}\\ -\frac{\exp(\lambda_3T_s)-1}{2\lambda_3} & -\frac{L_{fc}\left[\exp(\lambda_3T_s)-1\right]}{2L_{fg}\lambda_3}\end{bmatrix},$$

$\bar{\mathbf{C}}_d=\bar{\mathbf{C}}$, $\bar{\mathbf{D}}_d=\bar{\mathbf{D}}$, T_s stands for sampling time.

The results in (8) is simpler and more stable than the discretized system with ZOH method from original system in [8] or [9]. The internal stability and oscillation of discrete system of original one will be discussed in Section IV.

III. Observer and Controller Design

A. Observer design

The gains of state observer can be calculated in both continuous and discrete time domain. The gains in continuous domain are presented in Appendix, and these gains should be properly transformed to discrete time domain. Instead, direct design in the discrete time domain is proposed. The difference equation of discrete state observer is given by (9) where $\mathbf{L}_d=\left[L_{d1}\quad L_{d2}\quad L_{d3}\right]^T$, and the characteristic polynomial of the error dynamics is given by (10). Although the poles can be directly selected in *z*-domain, the poles are selected in *s*-domain in advanced for physical insight. One real pole (ω_o) and conjugate complex poles (β and $\beta*$) have been selected. The complex poles represent dynamics of $s^2+2\zeta_{o2}\omega_{o2}s+\omega_{o2}^2$. The *s*-domain poles are translated to the *z*-domain pole using $z=\exp(sT_s)$ as (11).

$$\bar{\mathbf{x}}_h[k+1]=\bar{\mathbf{A}}_d\bar{\mathbf{x}}_h[k]+\bar{\mathbf{B}}_d\mathbf{u}[k]+\mathbf{L}_d\left(\mathbf{y}[k]-\bar{\mathbf{C}}_d\bar{\mathbf{x}}_h[k]\right) \tag{9}$$

$$\det\left(z\mathbf{I}-\bar{\mathbf{A}}_d+\mathbf{L}_d\bar{\mathbf{C}}_d\right)=(z-z_0)(z-z_1)(z-z_2) \tag{10}$$

$$z_0=\exp(\omega_0T_s)$$
$$z_1=\exp(\beta T_s) \tag{11}$$
$$z_2=\exp(\beta*T_s)$$

The observer gains can be calculated by solving (12).

$$\begin{bmatrix}-1 & 1 & -1\\ z_{\lambda2}+z_{\lambda3} & -(z_{\lambda1}+z_{\lambda3}) & z_{\lambda1}+z_{\lambda2}\\ -z_{\lambda2}z_{\lambda3} & z_{\lambda1}z_{\lambda3} & z_{\lambda1}z_{\lambda2}\end{bmatrix}\begin{bmatrix}\bar{L}_{d1}\\ L_{d2}\\ \bar{L}_{d3}\end{bmatrix}=\begin{bmatrix}Z_2-W_2\\ Z_1-W_1\\ Z_0-W_0\end{bmatrix} \tag{12}$$

where, $Z_2=-(z_0+z_1+z_2)$, $Z_1=z_0z_1+z_1z_2+z_2z_0$, $Z_0=-z_0z_1z_2$, $W_2=-(z_{\lambda1}+z_{\lambda2}+z_{\lambda3})$, $W_1=z_{\lambda1}z_{\lambda2}+z_{\lambda2}z_{\lambda3}+z_{\lambda3}z_{\lambda1}$, $W_0=-z_{\lambda1}z_{\lambda2}z_{\lambda3}$, $z_{\lambda1}=\exp(\lambda_1T_s)$, $z_{\lambda2}=\exp(\lambda_2T_s)$, $z_{\lambda3}=\exp(\lambda_3T_s)$, and $L_{d1}=L_{fc}L_{fg}^{-1}\bar{L}_{d1}$, $L_{d3}=L_{fc}L_{fg}^{-1}\bar{L}_{d3}$.

The pole of observer can be placed at a higher frequency than the current control dynamics and lower than the Nyquist frequency. But it is not necessary to set higher than the filter resonant frequency.

B. Controller design

As mentioned before, although both converter current and grid current can be used for feedback, the resonant frequency of LCL filter affects to the stability of the control. If the resonant frequency is set over 1/6 and under 1/2 of sampling frequency, the grid current control is stable without active damping. However, in some case, the current sensor should be installed at the output of converter due to the package consideration. As a result, the resonant frequency should be set under 1/6 of sampling frequency for stable current regulation without active damping. But the size of filter should be getting larger, or the active damping implementation can increase number of sensors.

In this paper, the grid current estimated by state observer is fed back to regulator. The resonant frequency of LCL filter is set over 1/6 of sampling frequency with fulfillment for current harmonic restrictions. The stable current regulation is satisfied and the filter size is getting smaller. Because the resonant frequency is designed much larger than current regulation dynamics, the LCL filter can be approximated to L filter in the view point of current control [1]. The conventional synchronous reference frame PI (Proportional and Integral) regulator can be adopted and the gains can be set to achieve the first order low-pass filter dynamics as (13). The cut-off frequency of current controller, ω_{cc}, should be set under 1/10 to 1/6 of observer poles.

$$k_p=L_{f,sum}\omega_{cc}$$
$$k_i=\left(R_{fc}+R_{fg}\right)\omega_{cc} \tag{13}$$

C. Considerations for digital implementation

The delay due to PWM and digital control used to be considered for control loop design, and it affects to the observer design. With a proper compensation such as in [14], this delay can be effectively compensated. In this case, the output of PI controller directly used for state observer input, and it is not necessary to change observer gain due to the digital delay. The output of controller at time ‘k-1’ becomes input of state observer at time ‘k’.

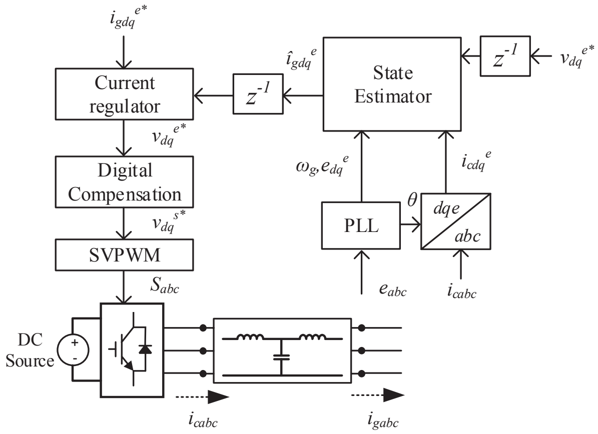

Fig. 3. Proposed control scheme

The proposed control scheme considering digital implementation is depicted in Fig. 3. The estimated grid currents of state observer at 'k-1' are fed-back to current regulator, and the output of controller at 'k-1' used for state estimation in the next sample period.

IV. Verification

A. Open loop test

The open loop response of proposed diagonal system has been evaluated, and Fig. 4 shows the results. Three systems have been tested.

(a) original state equation in (1) in *continuous* time domain,

(b) state equation in [8] or [9] in *discrete* time domain,

(c) proposed state equation in *discrete* time domain.

The values of system (b) were labeled as 'estimated *variable* (1)', and the values of system (b) as 'estimated *variable* (2)'.

Input (converter) voltages were set to operate system in rated power condition. The input is set to nominal grid voltage before applying step input, so both *d* and *q*-axis currents were kept zero. At 0.1 s, the *d*-axis voltage is applied in advance, and the *q*-axis voltage is applied at 0.2 s. System (b) shows oscillation after input was applied, but proposed system (c) has no oscillation for open loop test and shows the same dynamics to the original system. These imply that, in the view point of internal stability, proposed diagonal state equation is internal stable even in discrete time domain, but the discrete state equation with lossless is unstable internally. Although the state observer can cancel such unstable poles by unstable zeros and the unstable poles seem to disappear form the system, the unstable poles still there and can invoke instability. The proposed asymptote poles make system internally stable, and such problem will not appear.

B. Closed loop control

Fig. 5 shows the results of conventional closed loop current control with converter current feedback without state observer.

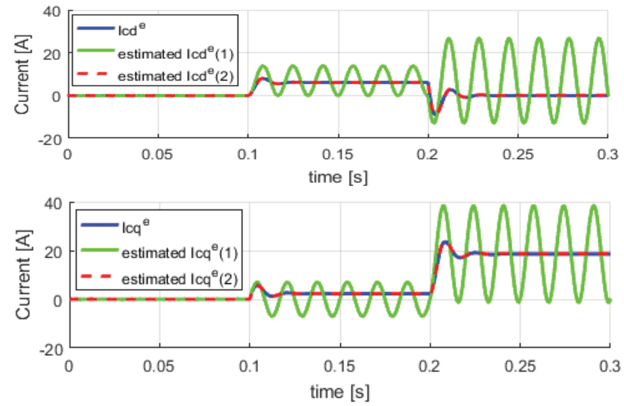

(a) Converter currents

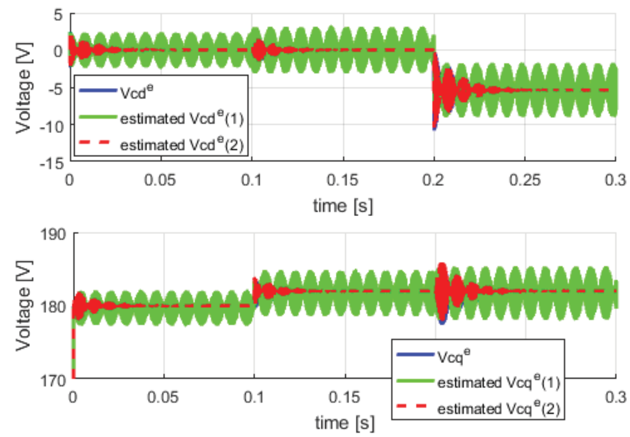

(b) Filter capacitor voltage

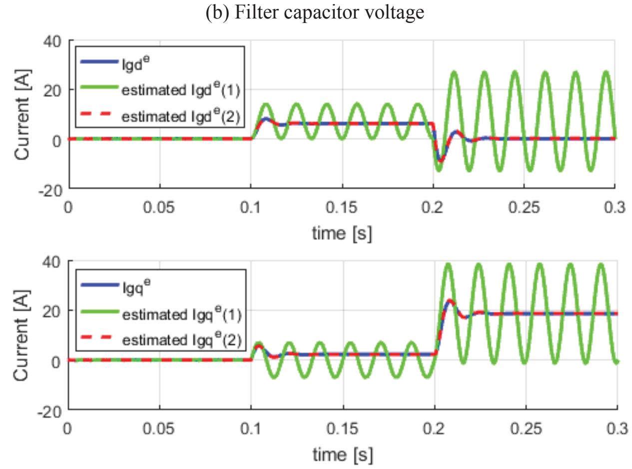

(c) Grid currents

Fig. 4. Open loop test results for state equations

The current control cut-off frequency is sot to 200 Hz. The system can operate stably if the f_{res} / f_{samp} is under 1/6. In the contrast, the f_{res} / f_{samp} beyond 1/6 made system unstable, and the voltages and currents at PCC (point of common coupling) were diverged right after PCS started switching operation.

Fig. 6 and 7 shows the result for proposed control scheme, and the resonant frequency of LCL filter is same to Fig. 5 (b).

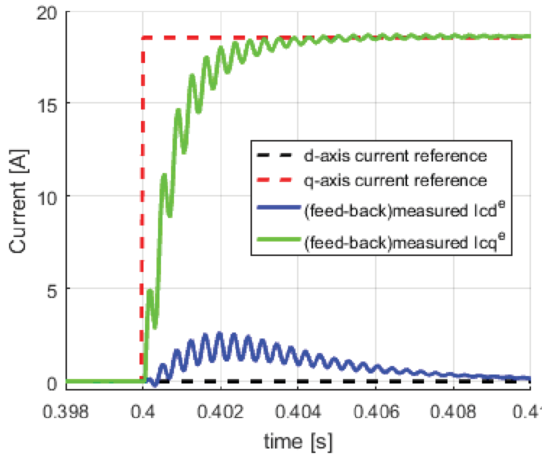

(a) f_{res} = 2.5 kHz < 1/6 f_{samp}

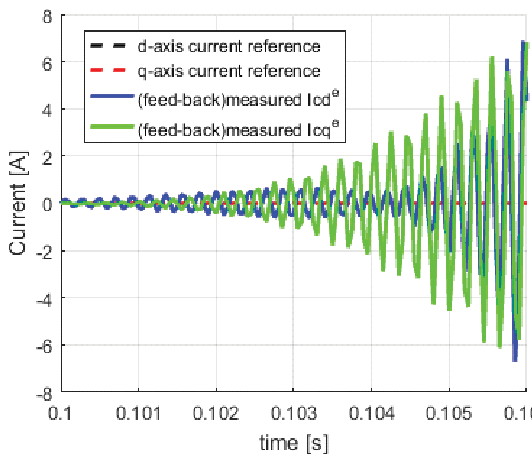

(b) f_{res} = 4.5 kHz > 1/6 f_{samp}

Fig. 5. Closed loop current control test results according to the LCL filter resonant frequency

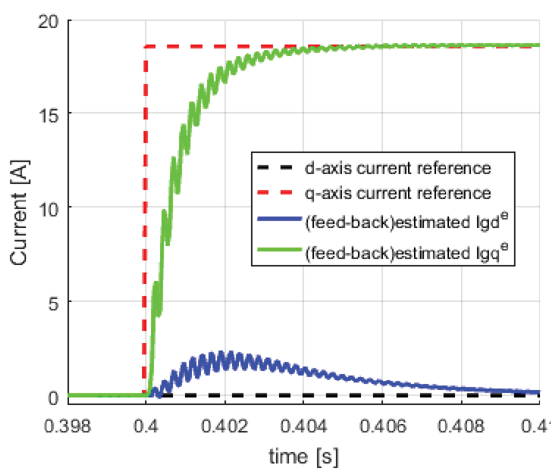

Fig. 6. Closed loop current control test results of proposed control scheme (f_{res} = 4.5 kHz > 1/6 f_{samp})

Although the hardware is identical, proposed scheme can stabilize the system without additional sensors as in Fig. 5. Fig. 6 show the estimated states are well tracking measured states in operation.

V. Conclusions

This paper presents control scheme to operate PCS with converter current feedback without active damping. LCL filter has the resonant frequency beyond 1/6 of sampling frequency, and it was known that this condition makes converter current feedback system unstable without additional sensors. The proposed control scheme was adopted state observer, and the estimated currents were fed-back to current regulator. The discrete state equation with diagonal system matrix was derived by similar transformation and ZOH method. The asymptote eigenvalues were proposed for diagonal elements. These can make system internally stable, alleviate the oscillations in open loop system, and demonstrate the original system. The direct discrete observer design was implemented.

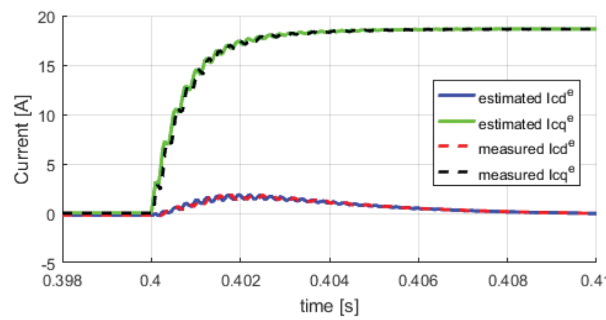

(a) Converter currents

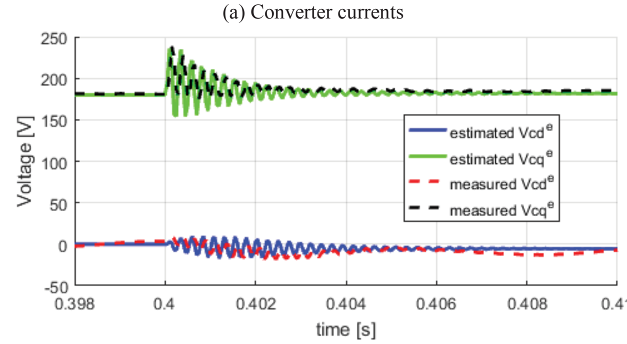

(b) Filter capacitor voltage

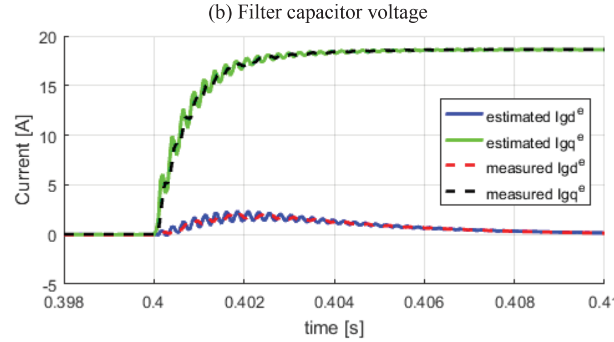

(c) Grid currents

Fig. 7. State estimation results with closed loop current control (f_{res} = 4.5 kHz > 1/6 f_{samp})

APPENDIX

The state observer can be set by both continuous and discrete time domain. The observer gain matrix, $\overline{\mathbf{L}} = \begin{bmatrix} \overline{L}_1 & \overline{L}_2 & \overline{L}_3 \end{bmatrix}^T$, in continuous time domain is given by (A1). The characteristic polynomial of the error dynamics is designed as (A2). One real pole and conjugate complex pole have been selected.

$$\begin{aligned} \overline{L}_1 &= \frac{L_{fc}}{L_{fg}}\left[\frac{1}{2}\frac{T_0}{\omega_p^2} - T_2 + \frac{1}{j\omega_p}\left(T_1 - \omega_p^2\right)\right] \\ \overline{L}_2 &= \frac{T_0}{\omega_p^2} \\ \overline{L}_3 &= -\overline{L}_1 + \frac{L_{fc}}{L_{fg}}\left(\overline{L}_2 - T_2\right) \end{aligned} \quad \text{(A1)}$$

where, $T_0 = \left(\omega_{o1} - j\omega_g\right)\left(-\omega_g^3 + \omega_{o2}^2 - j2\omega_g\zeta_{o2}\omega_{o2}\right)$,
$T_1 = -3\omega_g^2 + \omega_{o2}^2 + 2\omega_{o1}\zeta_{o2}\omega_{o2} - j2\omega_g\omega_{o2}\left(2\zeta_{o2} + 1\right)$,
$T_2 = \omega_{o1} + 2\zeta_{o2}\omega_{o2} - j3\omega_g$.

$$\det\left(s\mathbf{I} - \overline{\mathbf{A}} + \overline{\mathbf{L}}\overline{\mathbf{C}}\right) = \left(s + \omega_{o1}\right)\left(s^2 + 2\zeta_{o2}\omega_{o2}s + \omega_{o2}^2\right) \quad \text{(A2)}$$

REFERENCES

[1] B.-G. Cho, S,-K. Sul, H. Yoo, and S.-M. Lee, "LCL filter design and control for grid-connected PWM converter," in *Proc. 8th Int. Conf. on Power Electron. and ECCE Asia*, 2011, pp. 756-763.

[2] M. Romdhance, M. Naouar, I. Belkhodja, and Eric Monmasson, "Robust active damping methods for LCL filter-based grid-connected converters," PE, vol. 32, no. 9, pp 6739-6750, Sept 2017.

[3] B.-G. Cho, and S,-K. Sul, "LCL filter design for grid-connected voltage-source converters in high power systems," ECCE 2012.

[4] W. Yao, Y. Yang, X. Zhang, F. Blaabjerg, and P. Loh, "Design and analysis of robust active damping for LCL filters using digital notch filters," PE, vol. 32, no. 3, pp. 2360-2375, Mar. 2017.

[5] J. Wang, J. Yan, L. Jian, and J. Zou, "Delay-dependent stability of single-loop controlled grid-connected inverters with LCL filters," PE, vol. 31, no. 1, pp. 743-757, Jan 2016.

[6] Y. Tang, C. Yoon, R. Zhu, an dF. Blaabjerg, "Generalized stability regions of current control for LCL-filtered grid-connected converters without passive or active damping," in *Proc. IEEE Energy Convers. Congr. and Expo (ECCE),* 2015, pp. 2040-2047.

[7] S. Parker, B. P. McGrath, and D. G. Holmes, "Regions of active damping control for LCL filters," *IEEE Trnas. Ind. Appl.*, vol. 50, no. 1, pp. 424-432, Jan/Feb 2014.

[8] J. Kukkola, M. Hinkkanen, and K. Zenger, "Ovserver-based state-space current controller for a grid converter equipped with an LCL filter: analytical method for direct discrete-time design," *IEEE Trnas. Ind. Appl.*, vol. 51, no. 5, pp. 4079-4090, Setp/Oct. 2015.

[9] V. Miskovic, V. Blasko, T. M. Jahns, A. Smith, and C. Romenesko, "Obesrver-based active damping of LCL resonance in grid-connected voltage source converters," *IEEE Trnas. Ind. Appl.*, vol. 50, no. 6, pp. 3977-3985, Nov/Dec. 2015.

[10] B. Kim and S.-K. Sul, "Stability oriented design of frequency drift anti-islanding and phase-locked loop under weak grid," *IEEE J. Emerg. Sel. Topics Power Electron.*, vol. 5, no. 2, pp 760-774, Jun. 2017.

[11] A. Veloni, and N. Miridakis, *Digital control systems: theoretical problems and simulation tools*, CRC Press, Boca Raton, 2018.

[12] C. Chen, *Linear system theory and design*, Oxford Univ. Press, NY Oxford, 1999.

[13] S. Friedberg, A. Insel, and L. Spence, *Linear algebar*, Prentice Hall, 1997.

[14] B.-H. Bae and S.-K. Sul, "A compensation method for time delay of full-digital synchronous frame current regulator of PWM ac drives," *IEEE Trans. Ind. Appl.*, vol. 39, no. 3, pp. 802-810, May/June 2003.